

THE INFRARED [WC] STARS

ALBERT A. ZIJLSTRA
The University of Manchester
Manchester M13 9PL, UK

(First published in *Astrophysics & Space Science*, 275, 90 (2001). Some references to more recent works have been added as footnotes to the original text)

Abstract. A number of late [WC] stars have unique infrared properties, not found among the non-[WC] planetary nebulae, and together define a class of IR-[WC] stars. They have unusual IRAS colours, resembling stars in the earliest post-AGB evolution and possibly related to PAH formation. Most or all show a double chemistry, with both a neutral (molecular) oxygen-rich and an inner carbon-rich region. Their dense nebulae indicate recent evolution from the AGB, suggesting a fatal-thermal-pulse (FTP) scenario. Although both the colours and the stellar characteristics predict fast evolution, it is shown that this phase must last for 10^4 yr. The morphologies of the nebulae are discussed. For one object in Sgr, the progenitor mass ($1.3 M_{\odot}$) is known. The stellar temperatures of the IR-[WC] stars appear much higher in low metallicity systems (LMC, Sgr). This may be indicative of an extended 'pseudo' photosphere. It is proposed that re-accretion of ejected gas may slow down the post-AGB evolution and so extend the life time of the IR-[WC] stars.

1. Introduction

The nebulae surrounding the hydrogen-poor emission-line [WC] stars are thought not to differ from those surrounding non-[WC] stars, except for a higher expansion velocity (Gorny & Stasinska 1995) and higher internal turbulence (Gesicki et al. 1998), both of which can be understood as the effect of the hydrogen-poor wind on the nebula (Mellema, these pro-

ceedings). The lack of chemical peculiarities in the nebulae shows that the ejected occurred before the star became hydrogen poor. The normal range of ionized masses indicates that this occurred on the AGB, in a normal AGB superwind phase.

The hydrogen-poor nature of the [WC] star is probably related to a thermal pulse. This can have occurred during three possible phases: (1) on the white dwarf cooling track (a very late thermal pulse or VLTP); (2) during the hydrogen-burning post-AGB evolution (a late thermal pulse or LTP); (3) at the very end of the AGB, with the pulse terminating the AGB evolution (a fatal thermal pulse or FTP). The VLTP model is preferred from stellar modelling (e.g. Herwig et al. 1999). The nebulae surrounding VLTP [WC] stars should be highly evolved, since the pulse occurs $\sim 10^4$ yr after the AGB. The envelope mass of the star prior to VLTP is very small ($10^{-4} M_{\odot}$), and so the PN cannot be resupplied with significant amounts of hydrogen-rich gas. Some of the [WC] PNe are so compact that they must have been ejected on the AGB very recently. For these objects the FTP scenario may be preferred (Zijlstra et al. 1991).

The compact [WC] PNe are extremely bright infrared emitters. I will show that their nebulae have unexpected characteristics, and do not have a counterpart among non-[WC] PN.¹

2. Infrared flux and colours

Table 1 lists all known Galactic [WC] stars in the catalog of Gorny (these proceedings), with IRAS detections (flux quality 2 or 3) at 12, 25 and 60 micron. IRAS21282+5050 is included: although this object does not satisfy the [WC] criteria due to the lack of higher ionization levels (Crowther et al. 1998), it shows characteristics very similar to belong to the late [WC] stars. PC14 is not included: it has very peculiar IRAS colours but the IRAS position is more than 1 arcmin from the PN and confusion is likely. The total sample contains 40 objects. There is no excess of objects towards the Bulge suggesting all are Galactic disk objects.

Figure 1 shows the IRAS colour–colour diagram for the objects of Table 1. In Fig. 1a the 40 [WC] stars (filled circles) are shown together with all other PNe (open circles). The full PNe sample was selected as all PNe in the ESO-Strasbourg catalogue of PNe, with flux quality of 2 or 3 in all three bands, and where the IRAS position is within 20 arcsec of the optical position in the catalogue. The [WC] and other objects cover the same region of the diagram, but the [WC] stars are more predominant among the bluer

¹For a general recent review of planetary nebulae, published after these proceedings, see Kwitter & Henry 2022. A list of Galactic [WC] stars is in Muthumariappan & Parthasarathy 2020

TABLE 1. IRAS data for Galactic [WC] stars, in order of Galactic longitude

Name	[WC] subtype	F_{12} [Jy]	F_{25} [Jy]	F_{60} [Jy]	
SwSt1	9	17	86	24	IR-[WC]?
Cn1-5	4	1.7	7.5	9.4	
NGC6369	4	9.0	65.5	109	
Hb4	3.5	1.3	10.3	20.9	
M1-25	6	0.8	6.4	8.5	
M3-15	5	0.53	5.66	8.02	
M1-32	4.5	4.2	15.7	17.9	
PM1-188	11	3.8	15.3	14.8	
M1-61	4	2.19	26.5	17.0	
M1-60	4	0.5	5.6	8.5	
M1-51	5	3.6	23.3	31.4	
M2-43	8	15.7	53.8	21.3	IR-[WC]?
NGC6751	4	4.0	18.4	23.6	
He2-429	4.5	0.7	4.4	7.2	
PM1-310	11	2.1	8.4	6.0	
NGC6905	3	0.4	6.2	8.6	
BD+30°3639	9	89.4	234.5	161.7	IR-[WC]
He2-459	9	4.5	37.8	39.1	
NGC7026	3	2.4	18.4	42.7	
IRAS21282+5050	10	51.0	74.4	33.4	IR-[WC]
NGC40	8	14.5	71.9	64.8	
IC1747	4	0.7	3.7	8.2	
NGC1501	4	1.2	5.6	15.2	
M4-18	11	4.2	9.5	4.0	IR-[WC]?
IC2003	3	0.5	4.1	3.4	
NGC2452	3	0.5	5.0	6.6	
NGC2867	3	2.2	14.9	17.0	
PB6	3	0.92	6.0	5.1	
Pe1-1	4.5	1.8	18.4	11.9	
IRAS07027-7934	11	22.7	82.0	42.0	IR-[WC]
NGC5189	2	1.3	13.5	33.7	
He2-99	9	1.2	9.2	11.8	
NGC5315	4	7.5	72.0	84.0	
He2-113	11	92.4	310.5	176.6	IR-[WC]
PM1-89	4	2.3	12.9	14.2	
He2-142	9	13.8	31.0	15.6	IR-[WC]?
He3-1333	11	144.	257.	199.	IR-[WC]
Pe1-7	9	6.5	50.0	47.6	
K2-16	11	9.2	36.9	29.4	
IC1297	3	0.4	2.9	5.7	

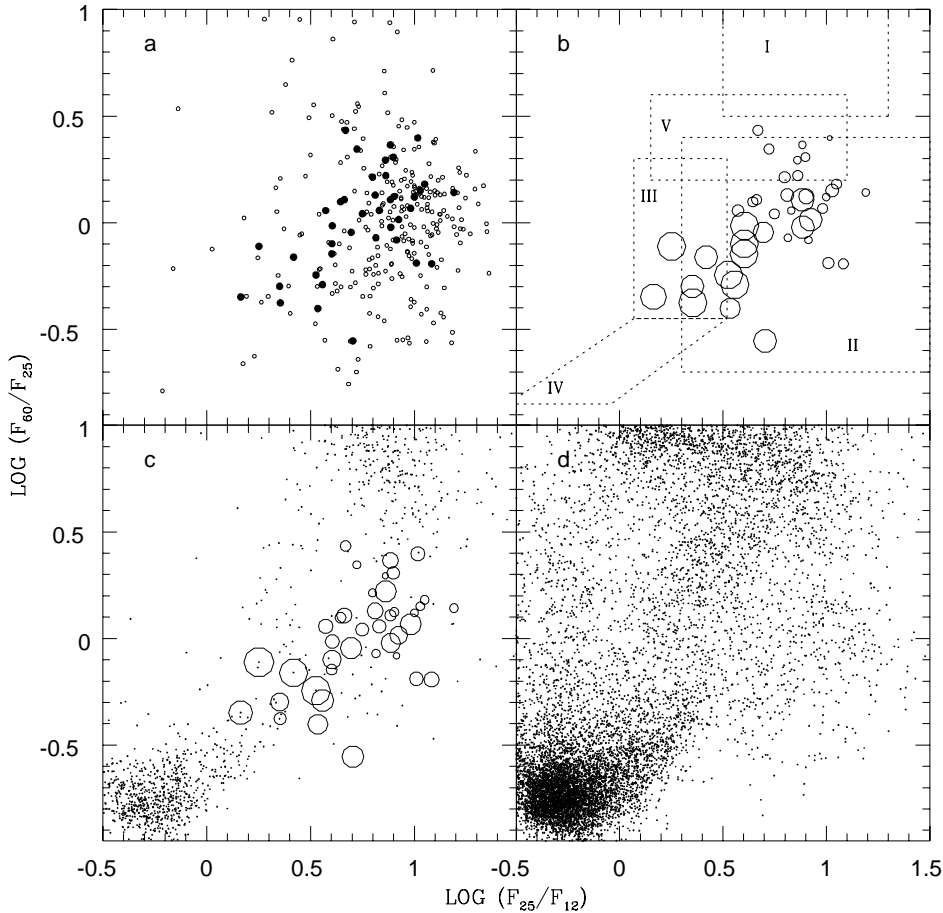


Figure 1. Infrared IRAS colours. The axes are defined in terms of $12\mu\text{m}$, $25\mu\text{m}$ and $60\mu\text{m}$ IRAS flux densities, without colour correction. Panel a: the open circles show all PNe detected in all three bands; the filled circles are all the [WC] stars. Panel b: the [WC] stars; the size of the circles is proportional to the subclass (class 11 are the largest circles). The boxes show the expected location of HII regions (I), PNe (II), PostAGB stars (III), Miras (IV) and bipolar outflow sources (V) (from Zijlstra et al. 2001). Panel c: the open circles are the [WC] stars; the size of the symbols is now proportional to the integrated IRAS flux. The dots represent all IRAS sources with integrated flux comparable to the IR-brightest [WC] stars. Panel d: All IRAS sources with good detections in all three bands.

objects. The [WC] stars have average IRAS colours of $(0.75, 0.01)$ in Fig. 1a, while the non-[WC] PNe have on average $(0.85, 0.02)$. Thus, the [WC] stars tend to have a relatively stronger F_{12} flux ratio but the F_{60}/F_{25} is no different. Sczcerba (these proceedings) shows that ISO spectra of some [WC] objects show faint PAH features: these could raise the 12-micron flux

and cause a blueward shift in the diagram. It thus appears that the dust characteristics differ between [WC] and non-[WC] stars.

Figure 1b shows the IRAS colours as function of [WC] subclass, where the size of the circles is proportional to the [WC] subclass; i.e. the largest circles correspond to the coolest central stars. The coolest stars have the hottest dust, implying their dust is nearest to the star. This agrees with a general evolution towards hotter stars while the nebula expands: the [WC] stars evolve towards higher temperatures on time scale comparable to the nebular expansion. The difference in distribution in Fig. 1a appears to be caused by the cooler [WC] stars only.

The boxes in Fig 1b indicate the typical location of different classes of objects, as indicated in the Figure caption. The [WC] stars are found on the blue side of the PNe box (as discussed before), with several having colours typical for young Post-AGB stars, with nebular time scales of only a few hundred years. A few [WC] stars have a $60\text{-}\mu\text{m}$ excess which puts them in a region where objects with bipolar outflows are found (Zijlstra et al. 2001).

In Fig. 1c the size of the open circles is proportional to the log of the integrated IRAS flux. The integrated flux is obtained by summing the in-band flux of the three bands and is thus a lower limit to the integrated dust emission, especially for hot objects. The objects with the hottest dust are also very bright in IRAS. This trend is affected by the unknown distances: the flux will scale with d^{-2} where d ranges from perhaps 1 kpc for the nearest objects to 8 kpc for Bulge nebulae. However, the dust emission declines so strongly as the nebula expands that the distance spread is a secondary parameter.

The dots in Fig. 1c are all entries in the IRAS point source catalogue with flux quality 3 at 12, 25 and $60\mu\text{m}$, and with total in-band flux $F_{ir} > 10^{-11} \text{ W m}^{-2}$ which is similar to the brightest [WC] stars. There are very few such IRAS sources especially in the PNe region, and those show colours clearly distinct from the [WC] stars. The bright [WC] stars form a well defined group among IRAS sources with little confusion with other types of objects. For comparison, Fig. 1d shows all IRAS sources with flux quality 3 at 12, 25 and $60\mu\text{m}$ (for all values of total flux). The AGB and its termination point are clearly visible, with the bright [WC] stars located near this point.

There is a gap in the distribution of bright IRAS sources in Fig 1c, at $(0.5, -0.3)$. This gap corresponds to the AGB–Post-AGB transition where evolution is extremely fast ($\sim 100\text{yr}$), when the envelope first becomes detached. The bright [WC] stars are seen to straddle this gap.

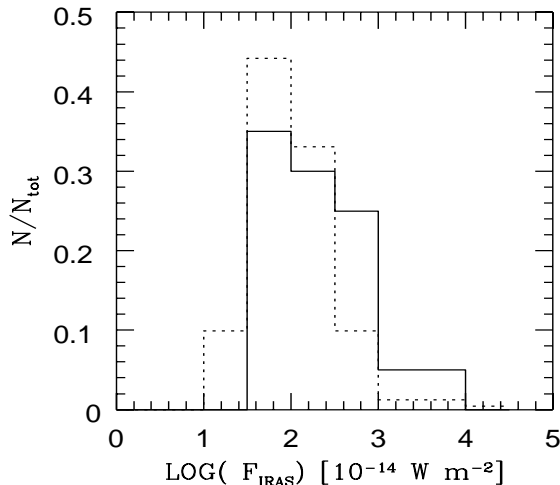


Figure 2. Histogram of the distribution of total in-band IRAS flux, for [WC] stars (drawn line) and other PNe (dashed line), for all objects with IRAS detections at 12, 25 and 60 μ m

3. Defining the IR-[WC] stars

Figure 2 shows the distribution of total in-band IRAS fluxes, with the drawn line representing the [WC] stars and the dashed line all non-[WC] PNe of Fig. 1a. The two distributions peak at a similar flux (10^{-12} W m⁻²), but the [WC] stars dominate at the highest integrated fluxes. The brightest IRAS PNe are almost all [WC] stars. These [WC] stars are the objects which are located near the post-AGB gap of Fig. 1c; all have late subtypes, or cool central stars. These are the IR-[WC] stars, defined as [WC] stars with IRAS in-band flux $F_{ir} > 0.8 \times 10^{-11}$ W m⁻² and IRAS colours near or in the post-AGB gap.

In Table 1, the IR-[WC] stars are indicated either as confirmed or possible. Confirmed stars (BD+30°3639, IRAS07027–7934, He 2-113 and He 3-1333 (also known as CPD–56°8032)) have colours near or in the gap and IRAS in-band flux $F_{ir} > 0.8 \times 10^{-11}$ W m⁻². The suspected candidates have similar colours but lower flux (possibly because of a larger distance). The [WC] subclasses range from 9 to 11, with one possible candidate (M2-43) having 8. This very limited range of subclass is not part of the selection criterion but indicates the likely common origin of the IR-[WC] stars.

Fig. 3 shows the IR-[WC] stars (filled circles), the possible ones (partly filled circles) and the other [WC] stars of Table 1 (open circles). The IR-[WC] stars very clearly separated from the other [WC] stars. The gap at

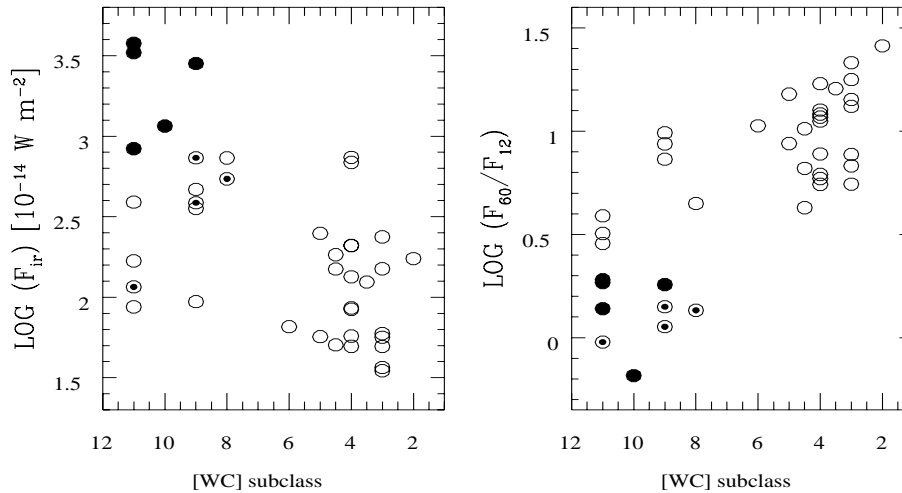


Figure 3. Total in-band IRAS flux and 60/12 micron colour versus [WC] subclass for the IR-[WC] stars (filled circles), possible IR-[WC] stars (half-filled circles) and other [WC] stars (open circles)

intermediate subclasses (5–7) is clear (Gorny & Stasinska 1995). The IR-[WC] stars all belong to the late [WC] stars. However, not all late [WC] stars belong to this class. Leaving out the IR-[WC] stars, the gap at subclasses 5–7 is much less significant.

The right panel effectively measures the distance in the colour–colour diagram from the AGB, showing the IR-[WC] stars should be in an extremely early post-AGB phase. These colours are however very different from those of the well-known bipolar post-AGB stars (such as, the Egg nebula and similar objects; Zijlstra et al. 2001) which are found near region V of Fig. 1b.

These IR-[WC] stars with colours similar to young post-AGB stars have few or no counterparts among the non-[WC] PNe. They define a separate class of objects, and point at a genuine difference in nebular evolution between some late [WC] stars and other PNe.

4. The silicate problem

Zijlstra et al. (1991) found an OH maser originating from the [WC11] star IRAS07027–7934. The IRAS LRS spectrum shows strong PAH features. This indicated a chemical dichotomy with both carbon-rich and oxygen-rich regions being present. The OH maser showed strong 1612MHz emission, a transition which requires long path lengths at moderate temperatures (Field

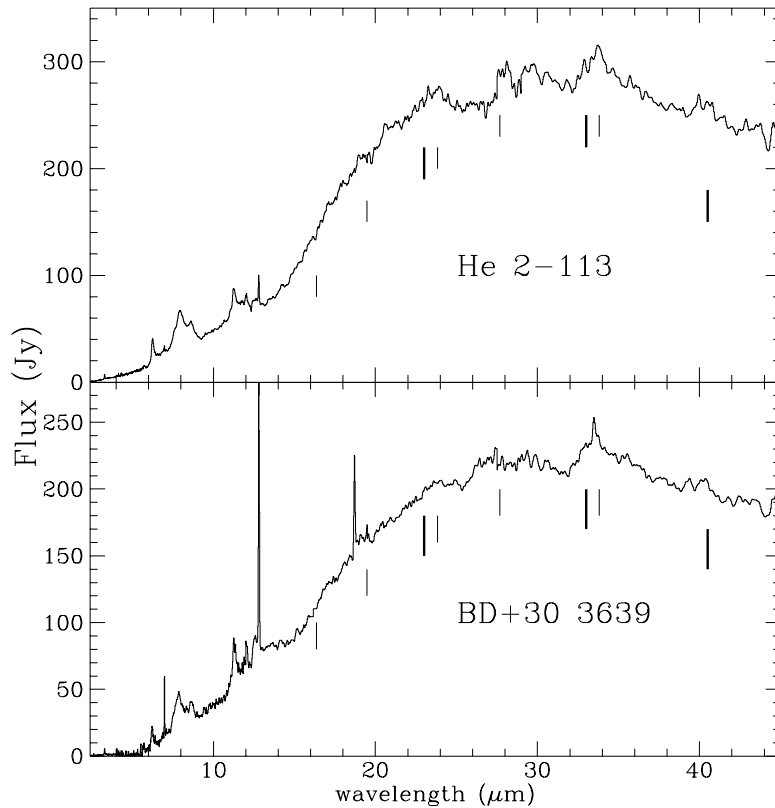


Figure 4. ISO spectra of two IR-[WC] stars, showing the PAH features at $\lambda < 13\mu\text{m}$, and the crystalline silicate bands at $\lambda > 20\mu\text{m}$. Thin marks indicate olivine bands and thick marks indicate pyroxenes (from Waters et al. 1998).

1985). The PAH emission requires a strong UV field. This implies that the oxygen-rich material is situated in the outer regions, while the carbon-rich dust is found close to the star. This was seen as evidence for a very recent (less than 500 yr ago) change of the star from oxygen to carbon rich, probably related to the thermal pulse. Thus, IRAS07027–7934 appears a candidate for a [WC] star which can only have formed through a fatal thermal pulse scenario.

Although previously a unique case, ISO spectroscopy found a similar chemical dichotomy in other [WC] stars, with strong PAHs bands at short wavelengths and bands of crystalline silicates (olivines and pyroxenes) at

longer wavelength. This has been seen in He 2-113 and BD+30°3639 (Waters et al. 1998) and in He 3-1333 (Cohen et al. 1998). The temperature of the crystalline dust is lower than the PAH particles, indicating there is a carbon-rich region close to the star but an oxygen-rich region at larger distances. In BD+30°3639 and He 3-1333 the ionized region is known to be strongly carbon rich and the likely seat of the PAH emission (Siebenmorgen et al. 1994). The chemical change in the stellar wind was dated to about 1000 yr ago for both He 2-113 and BD+30°3639, and 250 yr for He 3-1333, consistent with the estimates for IRS07027–7934. In all cases, the silicates appear to be located in the molecular part of the envelope.²

The observations show that probably all confirmed IR-[WC] stars show the double chemistry. IRAS 21282+5050 has not yet been observed at long wavelengths, but it also shows very strong PAH emission (Geballe et al. 1994).

Chemical dichotomy (showing both a carbon-rich and an oxygen-rich region) is very rare in post-main-sequence objects. Novae show this behaviour (Evans et al. 1997). The Red Rectangle (Waters et al. 1996) shows PAHs band and strong crystalline silicates. IRAS08005–2356 (Bakker et al. 1997, Zijlstra et al. 2001) shows carbon molecules and an OH maser. Both the last two stars are too cool to ionize their nebulae. They are binary stars with the crystalline silicates trapped in an ancient disk: they are probably not related in any way to the [WC] stars. Roberts 22 also has PAHs, an OH maser and crystalline silicates. It has an inner ionized region (Zijlstra et al. 2001) but is probably a supergiant (Molster, priv comm.). Among PNe, NGC 6302 has very weak PAH emission and crystalline features.

It appears likely that the presence in PNe of strong PAH features in combination with OH masers and/or crystalline silicates is uniquely related to the IR-[WC] stars.³

5. Time scales

The IR colours, the IR fluxes and the chemical dichotomy all point at very short time scales of the order of 10^2 – 10^3 yr. The apparent conclusion is that the IR-[WC] stars were on the AGB before that time. The time when the star became hydrogen-poor may be even more recent: BD+30°3639 shows evidence for hydrogenated PAHs (Waters et al. 1998) implying that

²For some relevant results after these proceedings were published (2001), see Toala et al. 2019, Guzman-Ramirez et al. 2015, Clayton et al. 2011, Garcia-Hernandez et al. 2008

³Work done since these proceedings have shown that weak PAH emission is common in planetary nebulae, both oxygen-rich and carbon-rich, but strong PAHs are rare and indicate carbon-rich nebulae: Cerrigone et al. 2009, Guzman-Ramirez et al. 2014. Although the IR-[WC] stars are strong PAH emitters, they do not appear to show fullerene emission: Otsuka et al. 2014

the PAHs formed after the star became carbon rich but before it became hydrogen poor.

Cohen et al. (1998) note that such short time scales are implausible from evolutionary considerations, and suggest that the silicate grains do not participate in the nebular expansion and date back to a much earlier epoch. Support for their argument comes from a separate reasoning: if the timescale are so short, the stars should evolve rapidly in the HR diagram. One would expect to see hotter stars with a similar chemical dichotomy. Such stars are not known. On the other hand, hydrogen-poor stars must have very low stellar envelope mass, and the cool [WC] stars have wind with very high mass-loss rates. (Note that the extreme C/O ratio of He 3-1333 and He 2-113 (de Marco et al. 1998) suggest a very low envelope mass (e.g. Frost et al. 1998)). Low envelope mass would lead to very fast evolution towards higher temperatures. The lack of hot IR-[WC] stars is therefore puzzling.

The number of IR-[WC] stars can be used to obtain limits on the evolutionary age of the IR-[WC] stars. The IRAS in-band flux is about $10^{-11} \text{ W m}^{-2}$ which corresponds to a luminosity of approximately $10^{29} d^2 \text{ W}$ where d is the distance in kpc. The in-band flux will underestimate the total IR flux typically by a factor of 2 for objects with hot dust. This gives $L_{\text{IR}} \approx 500 d^2 L_{\odot}$. The distance should be less than about 3 kpc for post-AGB luminosities. In fact distance estimates for IR-[WC] stars are mostly 1–2 kpc.

The local column density of PNe is about 25 kpc^{-2} (Zijlstra & Pottasch 1991). The IR-[WC] PNe account for 1–2% of all PNe. For a life expectancy of $3 \times 10^4 \text{ yr}$ for a PN (Zijlstra & Pottasch 1991), we can expect one object within 2 kpc for every 100-yr phase of PN evolution. The number of IR-[WC] stars than implies a minimum life time of 500–1000 yr for a IR-[WC] PN if *all* PNe pass through this phase. The observed fraction of [WC] stars (8%) can be used as an upper limit to the fraction of PNe which may have been IR-[WC] stars. We find a *minimum* life time for an IR-[WC] star of $5 \times 10^3 \text{ yr}$, with a likely life time in excess of 10^4 yr .

This is in contradiction with the implied short nebular time scales, and agrees with the suggestion of Cohen et al. The discrepancy can be reduced by assuming a higher distance and luminosity for the IR-[WC] stars. However, PNe with stellar luminosity $> 10^4 L_{\odot}$ are very rare and would evolve rapidly, again decreasing the expected numbers. The observed number of objects shows that IR-[WC] stars are comparatively long-lived. *Both nebulae and stars must evolve much slower during the IR-[WC] phase than their compact nebulae suggest.*

6. Morphology

A way to slow down evolutionary time scales of the nebulae is by assuming the existence of a slowly expanding torus or disk (e.g. Waters et al 1998). This would lead to bipolar morphologies, with possibly high velocities perpendicular to the torus.

BD+30°3639 is among the most spherically symmetric PNe known. However, Bryce & Mellema (1999) have shown that in fact it has a high-velocity bipolar outflow and thus is likely bipolar. The nebula is seen almost pole-on hiding its true structure.

CPD−56°8032 and He2-113 are very compact but HST images have been published by de Marco et al. (1997). Both show irregular but ring-like structures. The structures are consistent with bipolar geometries but do not prove it. Curiously, both objects show that the 'central' star is in fact located off-centre of the nebulosity. The ionized core of IRAS 07027−7934 has not been imaged, being subarcsecond. There are a few indications of asphericity (the split OH profile, the fact that the CO expansion velocity is half that of the OH, and the fact that the ionized core is not quite at the centre of the H α scattering halo, Zijlstra et al. 1991), but no conclusive evidence. IRAS 21282+5050 has a strong bipolar morphology (Bregman et al. 1992).⁴

The evidence is at present inconclusive, but bipolar, torus-like morphologies, are possible for the IR-[WC] nebulae; these would allow for slower nebular expansion. Note that similar bipolar morphologies are seen in 10–15% of PN (Manchado et al. 1996). Off-centre central stars are however very rare.

7. Extra galactic [WC] stars: the effect of metallicity

There are few or no Bulge [WC] stars in Table 1, as argued above. However, there are [WC] stars known in nearby galaxies of which three have IRAS detections: He2-436 in the Sagittarius dwarf spheroidal at 25 kpc (Sgr: Zijlstra & Walsh 1996), and SMP 58 and SNP61 in the LMC (Zijlstra et al. 1994). Their IRAS data is listed in Table 2 where the flux densities for He 2-436 were re-determined using IRAS Software Telescope data (SRON, Groningen).

Sgr has a metallicity of $[Fe/H] = -0.55$ and a main-sequence turn-off mass of $1.3 M_{\odot}$ (Dudziak et al. 2000). Its two [WC] stars are the only such stars where these parameters are known.

The IR colours and IR flux (when scaled to a distance of 2 kpc) are similar to those of the IR-[WC] stars. However, Fig. 5 shows their [WC]

⁴More recent morphological work is in Garcia-Hernandez et al 2006

TABLE 2. IRAS data for extra-galactic [WC] stars

Name	[WC] subtype	F_{12}	F_{25}	F_{60}
He 2-436 (in Sgr)	3/4	0.22 Jy	0.49 Jy	0.11 Jy
SMP58 (in LMC)	4/5	0.15 Jy	0.22 Jy	–
SMP61 (in LMC)	4/5	0.08 Jy	0.13 Jy	<0.16 Jy

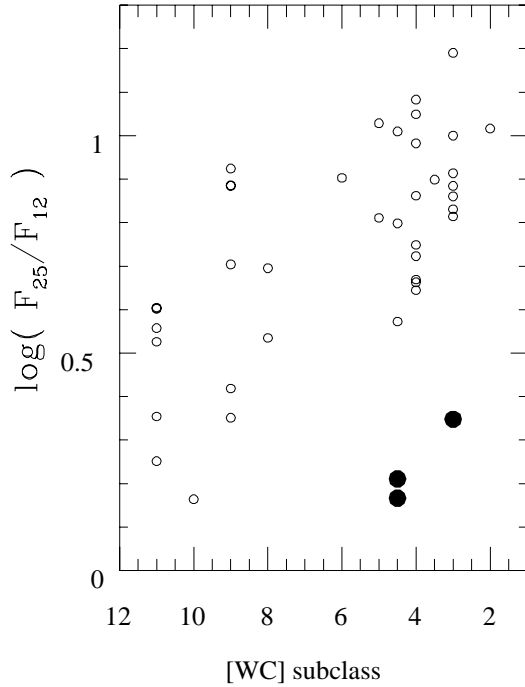


Figure 5. F_{12}/F_{25} as function of [WC] subclass, for Galactic [WC] stars (open circles), and the extra-galactic [WC] stars (filled circles)

subclass is much earlier than for Galactic stars with similar IR characteristics. Possibly the stars evolve faster to higher temperature at lower metallicity. Another possibility is that the subclass is affected by metal blanketing in an extended wind, in which case lower metallicity causes the $\tau = 1$ surface to be closer to the real stellar surface. (This would however imply that the late IR-[WC] stars have much hotter stars than the wind emission lines suggest.)

The data suggests that the group of the IR-[WC] stars is not confined

to the Galactic disk. However, the detailed properties show a dependence on metallicity. Given the AGB populations of Sgr and the LMC, it is likely that their progenitor stars were already carbon-rich before the ejection of the PN on the AGB. A chemical dichotomy similar to the Galactic IR-[WC] stars is therefore not expected.

8. The problem of evolution

There are three main problems regarding the IR-[WC] stars: (1) A unique nebular double chemistry seen *only* around IR-[WC] stars; (2) The conflict between the very short time scales implied by the nebulae and by the low envelope mass expected for a hydrogen-poor Post-AGB star, and the much longer timescales implied by other considerations; (3) The fact that the dense nebulae favour a fatal-thermal pulse (FTP) scenario whereas stellar model calculations favour a VLTP to obtain hydrogen-poor stars.

Long time scales require slow post-AGB evolution of the star. Slow evolution is expected for stars with very low core mass. However, their luminosity would also be very low, which is not observed.

The only other way to ensure slower post-AGB evolution is by replenishing the envelope of the star, to compensate for the effects of nuclear burning and wind mass loss. This would require accretion of mass from the ejecta back onto the star.

An accretion scenario could explain the link between dense, compact nebulae and the peculiar evolution. It requires that the hydrogen is efficiently mixed down in the star to maintain the [WC] characteristics. In such a model, the PAHs molecules could in fact form in the accreting gas, where CO is dissociated (as in novae, Evans et al. 1997). Furthermore, slow accretion could trigger a VLTP on the cooling track where otherwise this might not occur.

Such a model is highly speculative. It is however clear that the FTP and VLTP scenarios, while adequate for the other [WC] stars, do not as yet provide a good explanation for the IR-[WC] stars.

References

- Bakker E.J., van Dishoeck E.F., Waters L.B.F.M., Schoenmaker T., 1997, *A&A*, 323, 469
 Bregman J.D., Booth J., Gilmore D.K., Kay L., Rank D., 1992, *ApJ*, 396, 120
 Bryce M., Mellema G., 1999, *MNRAS*, 309, 731
 Cerrigone L., Hora J. L., Umana G., Trigilio C., 2009, *ApJ*, 703, 585
 Clayton G. C., De Marco O., Whitney B. A., Babler B., Gallagher J. S., Nordhaus J., Speck A. K., et al., 2011, *AJ*, 142, 54.
 Cohen M., Barlow M.J., Sylvester R.J., Liu X.-W., Cox P., Lim T., Schmitt B., Speck A.K., 1998, *ApJ*, 513, L135
 Crowther P.A., De Marco O., Barlow M.J., 1998, *MNRAS*, 296, 367
 De Marco O., Crowther P.A., 1998, *MNRAS*, 296, 419

- De Marco O., Barlow M.J., Storey P.J., 1997, MNRAS, 292, 86
Dudziak G., Pequignot P., Zijlstra A.A., Walsh J.R., 2000, A&A, 363, 717
Evans A., Geballe T.R., Rawlings J.M.C., Eyres S.P.S., Davies J.K., 1997, MNRAS, 292, 192
Field D., 1985, MNRAS, 217, 1
Frost C.A., Cannon R.C., Lattanzio J.C., Wood P.R., Forestini M., 1998, 332, L17
García-Hernández D. A., Manchado A., García-Lario P., Cañete A. B., Acosta-Pulido J. A., García A. M., 2006, ApJ, 640, 829
Geballe T.R., Joblin C., D’Hendecourt L.B., Jourdain de Muizon M., Tielens A.G.G.M., Leger A., 1994, ApJ, 434, L15
Gesicki K., Zijlstra A.A., Acker A., Szczerba R., 1998, A&A, 329, 265
Górny S. K., 2001, Ap&SS, 275, 67
Gorny S.K., Stasińska G., 1995, A&A, 303, 893
Guzman-Ramirez L., Lagadec E., Wesson R., Zijlstra A. A., Muller A., Jones D., Boffin H. M. J., et al., 2015, MNRAS, 451, L1
Guzman-Ramirez L., Lagadec E., Jones D., Zijlstra A. A., Gesicki K., 2014, MNRAS, 441, 364
Herwig F., Blöcker T., Langer N., Driebe T., 1999, A&A, 349, 15
Kwitter K. B., Henry R. B. C., 2022, PASP, 134, 022001
Manchado A., Guerrero M.A., Stanghellini L., Serra-Ricart M., 1996, The IAC Morphological Catalog of Northern Galactic Planetary Nebulae
Mellema G., 2001, Ap&SS, 275, 147
Muthumariappan C., Parthasarathy M., 2020, MNRAS, 493, 730
Otsuka M., Kemper F., Cami J., Peeters E., Bernard-Salas J., 2014, MNRAS, 437, 2577
Siebenmorgen R., Zijlstra A.A., Krügel E., 1994, MNRAS, 271, 449
Szczerba R., Górny S. K., Stasińska G., Siódmiak N., Tyłenda R., 2001, Ap&SS, 275, 113
Toalá J. A., Ramos-Larios G., Guerrero M. A., Todt H., 2019, MNRAS, 485, 3360
Waters L.B.F.M., Beintema D.A., Zijlstra A.A., de Koter A., Molster F.J., Bouwman J., de Jong T. Pottasch S.R., de Graauw Th., , 1998, A&A, 331, L61
Zijlstra A. A., Chapman J. M., te Lintel Hekkert P., Likkell L., Comeron F., Norris R. P., Molster F. J., et al., 2001, MNRAS, 322, 280
Zijlstra A. A., Walsh J. R., 1996, A&A, 312, L21
Zijlstra A.A., Pottasch S.R., 1991, A&A, 243, 478
Zijlstra A.A., Gaylard M.J., te Lintel Hekkert P., Menzies J.W., Nyman L.-A., Schwarz, H. E. 1991, A&A, 243, L9
Zijlstra A.A., van Hoof P.A.M., Chapman J.M., Loup C., 1994, A&A, 290, 228